RESEARCH ARTICLE

Figures and figure supplements

Selective transduction and photoinhibition of pre-Bötzinger complex neurons that project to the facial nucleus in rats affects nasofacial activity

Mariana R Melo *et al*.

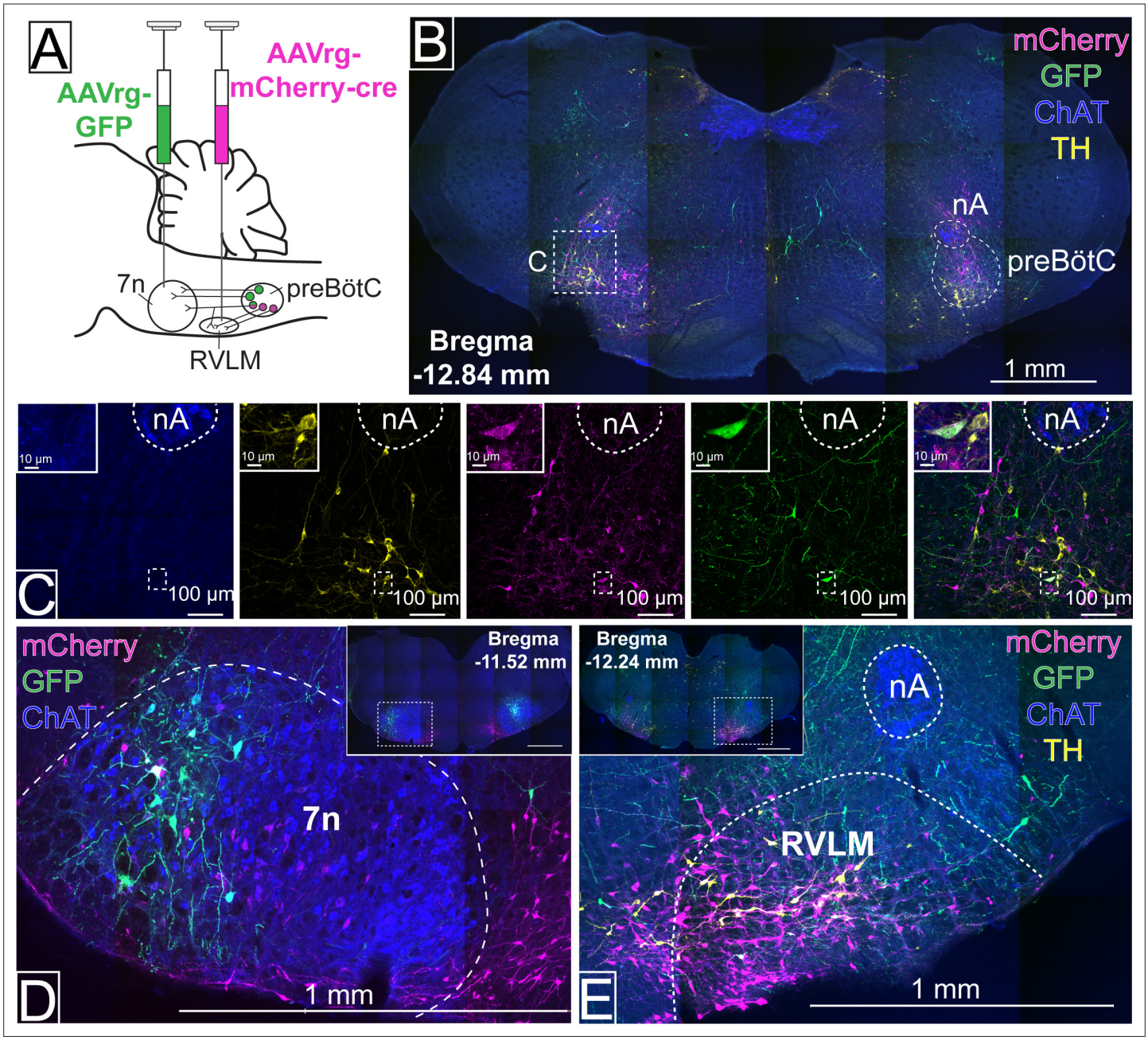

Figure 1. Distinct pre-Bötzinger complex (preBötC) subpopulations project to the facial nucleus (7n) and rostral ventrolateral medulla (RVLM). (**A**) Schematic diagram showing the dual retrograde viral strategy. (**B**) Coronal section showing preBötC neurons projecting to 7n (green) and RVLM (red). Tyrosine hydroxylase (TH; yellow) and choline acetyltransferase (ChAT; blue) neurons are shown. (**C**) Transduced preBötC neurons, highlighted in the hashed box in (**B**), shown in higher magnification. The inset shows a preBötC neuron that projects to both 7n and RVLM. Local transduction shows the 7n (**D**) and RVLM (**E**) injection sites. Abbreviations: nA: nucleus ambiguus.

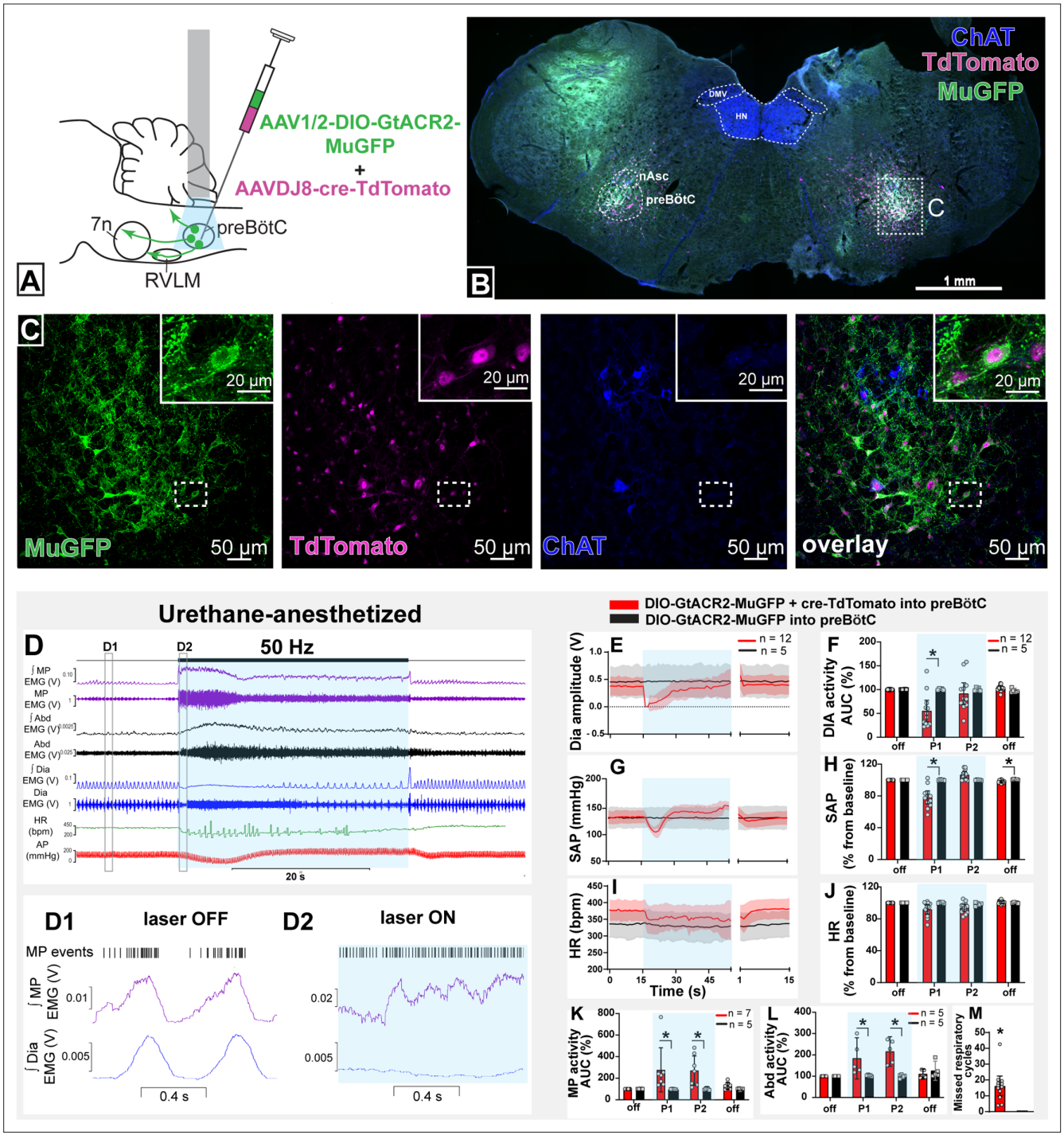

Figure 2. Effect on non-selective photoinhibition of pre-Bötzinger complex (preBötC) on cardiovascular, respiratory, and mystacial pad (MP) activity in urethane-anesthetized rats. (**A**) Schematic diagram showing the preBötC injection strategy. (**B**) Coronal section showing the expression of GtACR2-MuGFP and TdTomato in the preBötC, and choline acetyltransferase immunoreactivity (ChAT). Detailed maps showing the distribution of GtACR2-MuGFP expression are in ***Figure 2—figure supplement 1***. (**C**) Higher magnification confocal images of MuGFP and TdTomato in preBötC with the inset highlighting a double-labeled neuron. (**D**) Representative traces showing recordings of integrated (∫) and raw MP EMG, ∫ and raw abdominal muscle (Abd) EMG, ∫ and raw diaphragm (Dia) EMG, heart rate (HR), and arterial pressure (AP). Bilateral photoinhibition of preBötC, which occurs in the time highlighted by a blue box, produced increased, tonic MP and Abd activity, apnea, a biphasic change in AP, and decreased HR. Higher temporal resolution recordings of the periods highlighted by the hashed boxes are shown in (**D1**) and (**D2**), which show MP bursts as events, and triggered averages of ∫ MP and ∫ Dia EMG. Note that the inspiratory-related MP activity was interrupted by photoinhibition and MP EMG became increased and tonic. Group data showing mean (solid line) and 95% confidence intervals for (**E**) Dia amplitude, (**G**) systolic arterial pressure (SAP), (**I**) HR (bpm) before,

Figure 2 continued on next page

Figure 2 continued

during, and after photoinhibition in GtACR2 expressing (red) and control (black) rats. Histograms showing group data for the effect of photoinhibition of preBötC in respiratory and cardiovascular parameters (**F**) Dia amplitude, (**H**) SAP, (**J**) HR, (**K**) MP activity, (**L**) Abd activity, and (**M**) number of missed respiratory cycles; P1 and P2 refer to the initial period of photoinhibition, where apnea was complete, and the later period where breathing re-started respectively. The group data are presented as mean ± 95% CI; unpaired t-test or nonparametric Mann-Whitney test with multiple comparisons using the Bonferroni-Dunn method, *p<0.05. Abbreviations: nAsc: subcompact formation of the nucleus ambiguus; DMV: dorsal motor nucleus of the vagus; HN: hypoglossal nucleus. Control injections of AAV-DIO-GtACR2-MuGFP alone into preBötC are shown in ***Figure 2—figure supplement 2***.

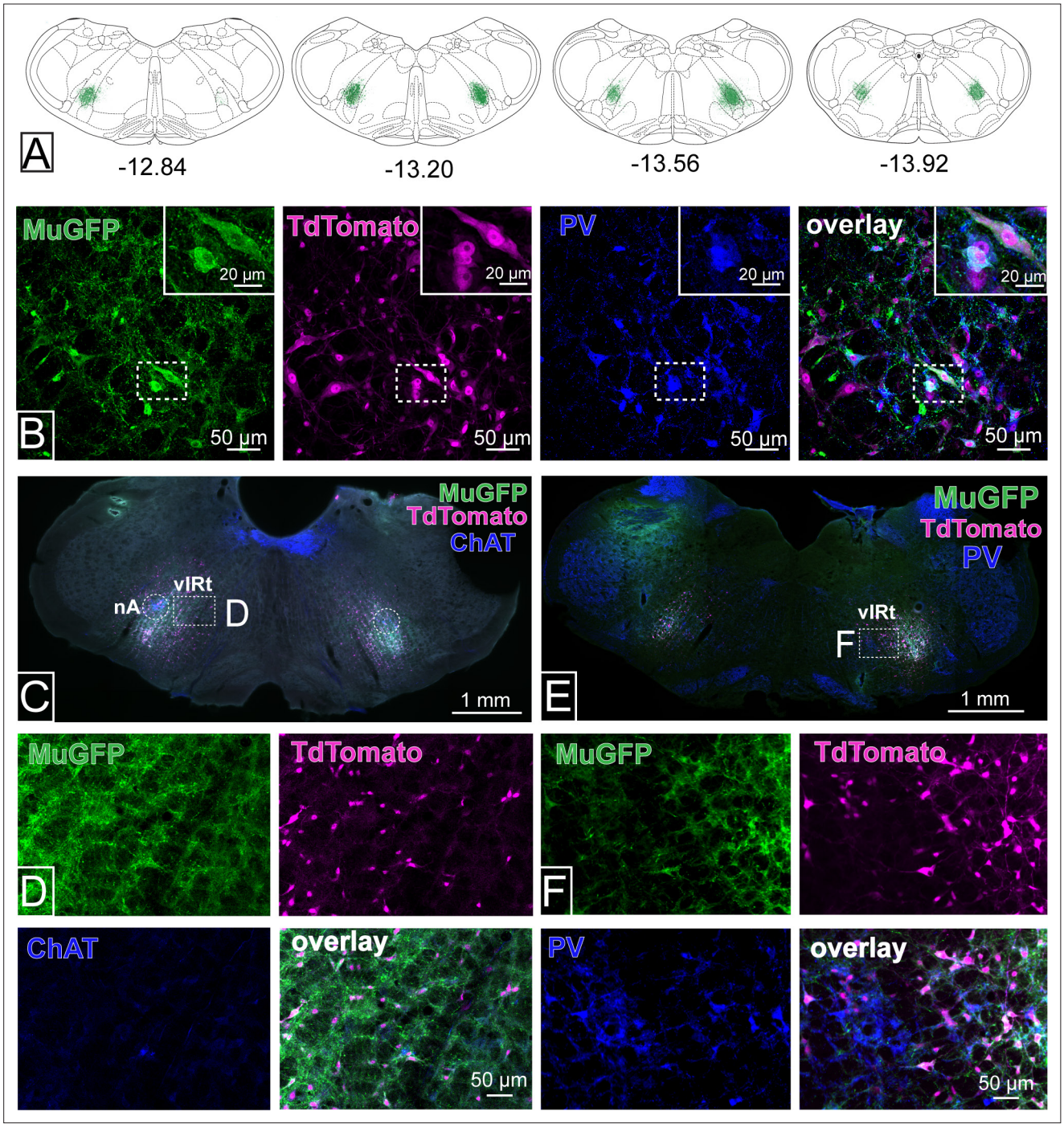

Figure 2—figure supplement 1. Expression of GtACR2-MuGFP in rats co-injected with AAV-DIO-GtACR2-MuGFP and AAVDJ8-Cre-TdTomato in the pre-Bötzinger complex (preBötC). (**A**) Schematic coronal sections of the rat medulla, based on the atlas of Paxinos and Watson, showing the superposition of neuronal labeling of GtACR2-MuGFP, at different rostrocaudal levels of the preBötC, shown relative to Bregma (mm), from a cohort of urethane-anesthetized rats (n=7). The distribution in each animal is shown, with increased intensity of the green depicting overlapping areas of transduction. Sections rostral or caudal to these levels had no labeling in any animal. (**B**) Viral transgene expression in parvalbumin (PV) expressing neurons of the rostral ventral respiratory group (rVRG). (**C, E**) Viral transgene expression in the vibrissa intermediate reticular nucleus (vIRt), which is located medially to nucleus ambiguus (nA) and depicted by a hashed boxes, in combination with immunohistochemistry for choline acetyltransferase (ChAT) (**C,D**) and parvalbumin (PV) (**E,F**). The hashed circles in (**C**) show the nA.

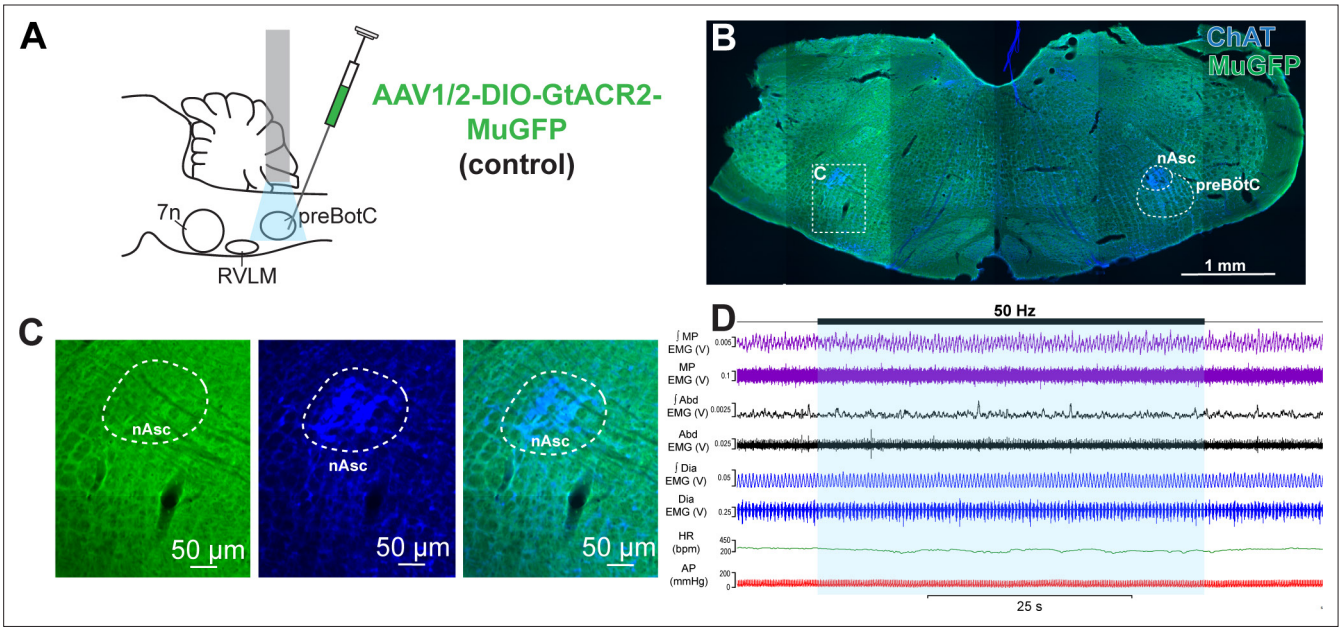

Figure 2—figure supplement 2. Control experiments with injection of AAV-DIO-GtACR2-MuGFP alone into pre-Bötzinger complex (preBötC). (**A**) Schematic diagram showing the injection protocol. (**B**) Coronal section showing that injection of AAV-DIO-GtACR2-MuGFP did not induce transgene expression in the preBötC. Immunoreactivity for choline acetyltransferase (ChAT) is used to show the position of the preBötC. (**C**) Higher magnification confocal image showing the absence GtACR2-MuGFP expression in the preBötC. (**D**) Representative trace showing the integrated (∫) and raw mystacial pad (MP) EMG, ∫ and raw abdominal muscle (Abd) EMG, ∫ and raw diaphragm (Dia) EMG, heart rate (HR), and arterial pressure (AP). The period of bilateral laser delivery into the preBötC is shown by the blue box. No changes in any of these parameters were observed in control rats. Abbreviation: nAsc: subcompact formation of the nucleus ambiguus.

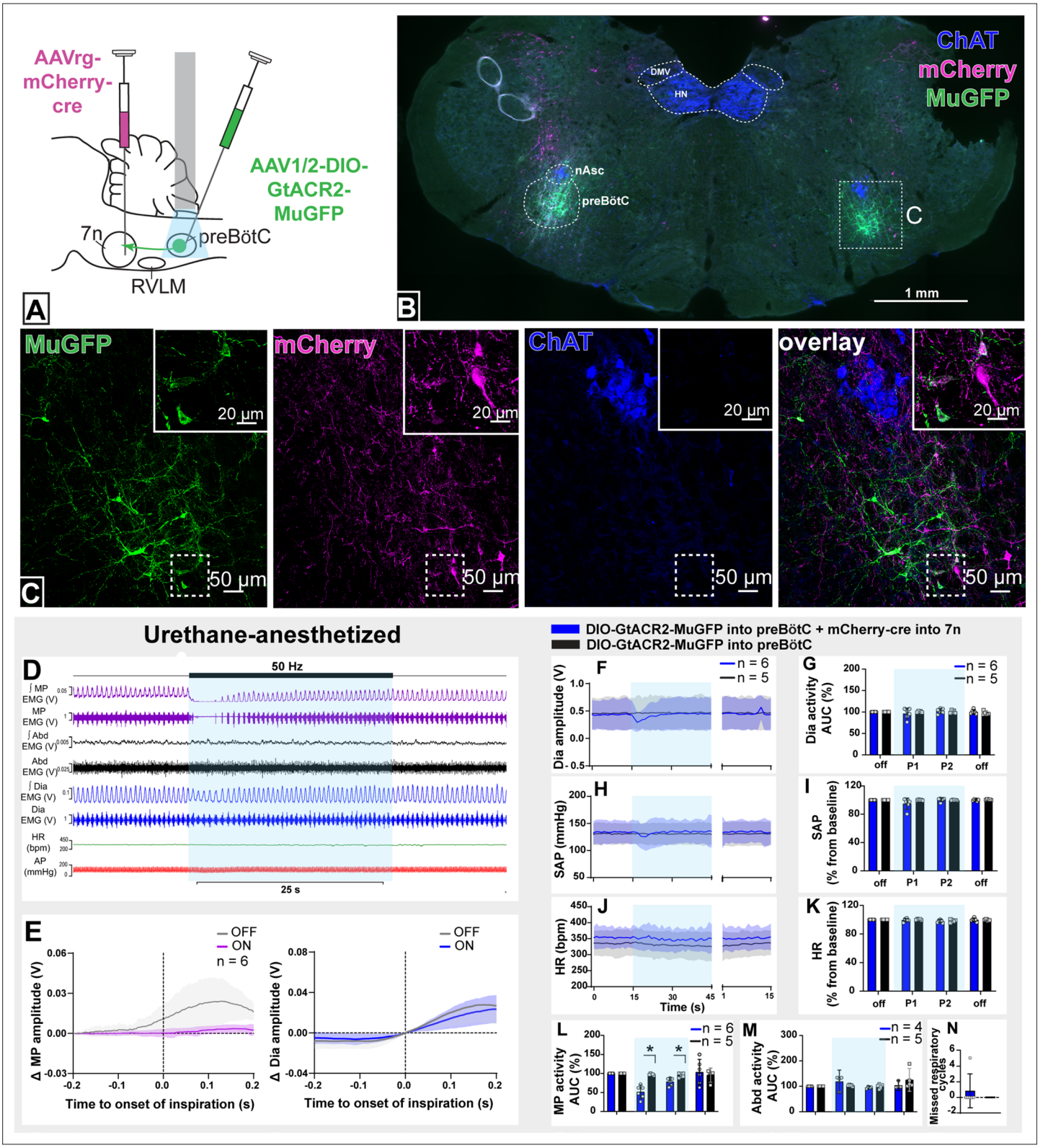

Figure 3. Effect of selective inhibition of pre-Bötzinger complex (preBötC)→7n neurons on cardiovascular, respiratory, and nasofacial activity in urethane-anesthetized rats. (**A**) Schematic diagram showing the injection protocol for selective transduction of preBötC→7n neurons. (**B**) Coronal section showing the expression of GtACR2-MuGFP and mCherry into the preBötC and immunohistochemistry for choline acetyltransferase (ChAT). Detailed maps showing the distribution of the expression of GtACR2-MuGFP are shown in ***Figure 3—figure supplement 1***. (**C**) Higher magnification confocal image showing the co-localization of MuGFP with mCherry in neurons of preBötC. (**D**) Representative trace showing the integrated (∫) and raw

Figure 3 continued on next page

Figure 3 continued

mystacial pad (MP) EMG, ∫ and raw abdominal muscle (Abd) EMG, ∫ and raw diaphragm (Dia) EMG, heart rate (HR), and arterial pressure (AP). Bilateral selective photoinhibition of preBötC→7n neurons, highlighted with the blue box, decreased the overall activity, and interrupted the inspiratory-related MP activity, with minimal effects on respiratory, cardiovascular, or abdominal muscle activity. (**E**) Event-triggered average showing the magnitude of inspiratory-related modulation of MP activity in the 150–200 ms before and after the onset of inspiration - denoted by the dotted line at time 0. Note that the inspiratory-related MP activity ceased, even in the absence of the interruption of inspiratory activity. Group data showing mean (solid line) and 95% confidence intervals for (**F**) Dia amplitude, (**H**) systolic arterial pressure (SAP), and (**J**) HR (bpm) before, during, and after photoinhibition in selective GtACR2 expressing (blue) and control (black) rats. Histograms showing group data for the effect of photoinhibition of preBötC on respiratory and cardiovascular parameters (**G**) Dia amplitude, (**I**) SAP, (**K**) HR, (**L**) MP activity, (**M**) Abd activity, and (**N**) number of missed respiratory cycles; P1 and P2 refer to the initial period of photoinhibition, where there is a small decrease in Dia amplitude and the later period respectively. Group data are presented as mean ± 95% CI; unpaired t-test or nonparametric Mann-Whitney test with multiple comparisons using the Bonferroni-Dunn method, *$p<0.05$. The period of photoinhibition of preBötC neurons is depicted by blue shading. Abbreviations: DMV: dorsal motor nucleus of the vagus; nAsc: subcompact formation of the nucleus ambiguus; HN: hypoglossal nucleus.

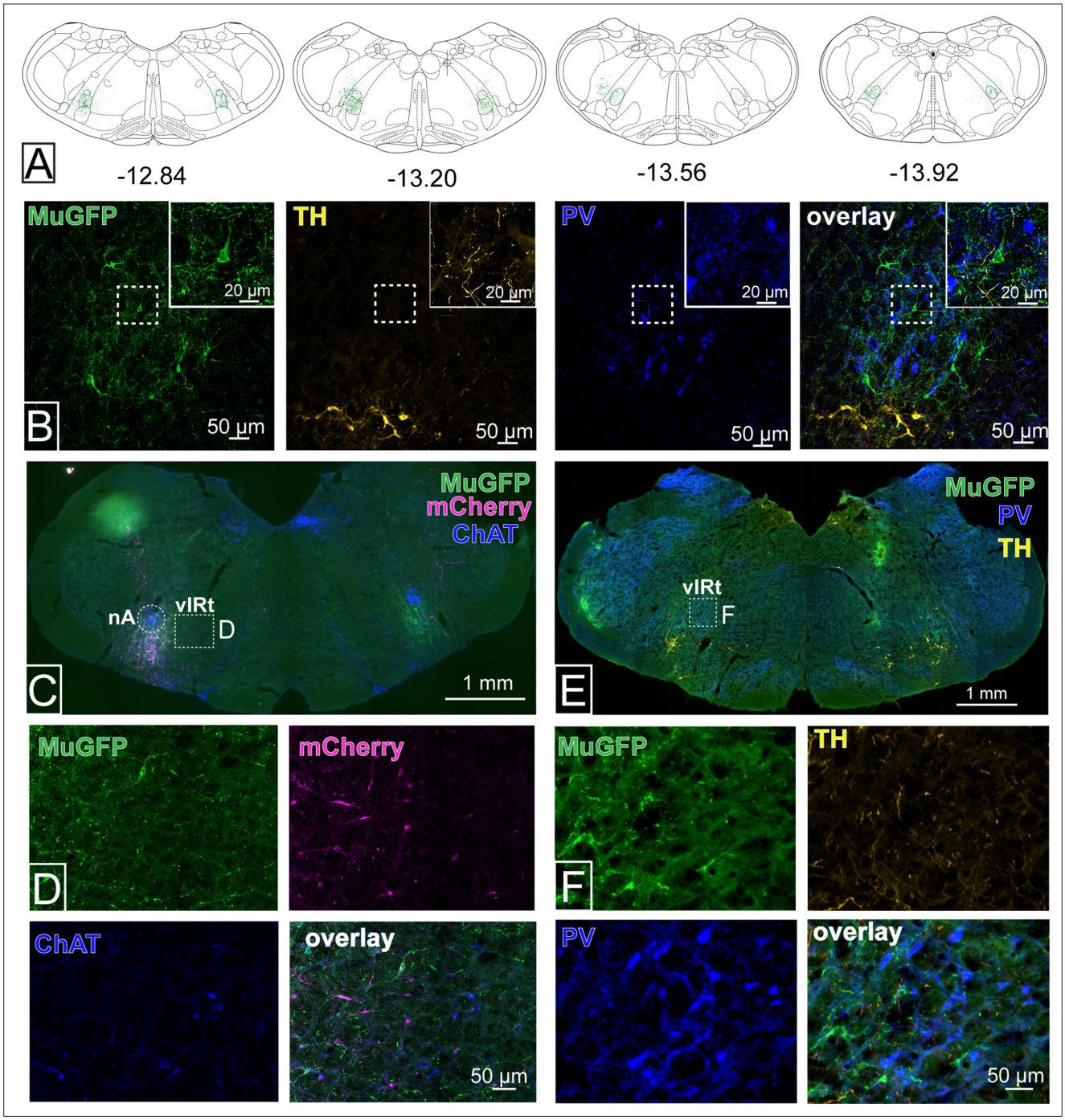

Figure 3—figure supplement 1. Expression of GtACR2-MuGFP in selective pre-Bötzinger complex (preBötC)→7n transduced rats. (**A**) Schematic coronal sections of the rat medulla, based on the atlas of Paxinos and Watson, 7ed., showing the superposition of neuronal labeling of GtACR2-MuGFP at different rostrocaudal levels of the preBötC, shown relative to Bregma (mm), from a cohort of urethane-anesthetized rats (n=5). The distribution in each animal is shown, with increased intensity of the green depicting overlapping areas of transduction. Sections rostral or caudal to these levels had no labeling in any animal. (**B**) GtACR2-MuGFP expression occurs in neurons intermingled with, but not co-expressing with, parvalbumin (PV) expressing neurons of the rostral ventral respiratory group (rVRG). Immunohistochemistry for tyrosine hydroxylase (TH; yellow) shows the ventrolateral medulla. (**C–D**) GtACR2-MuGFP expression in the vibrissa intermediate reticular nucleus (vIRt), which is located medially to nucleus ambiguus (nA), defined by expression of choline acetyltransferase (ChAT). (**E–F**) Parvalbumin-immunoreactive neurons of the vIRt are intermingled with, but separate from, transduced preBötC→7n neurons, and their processes.

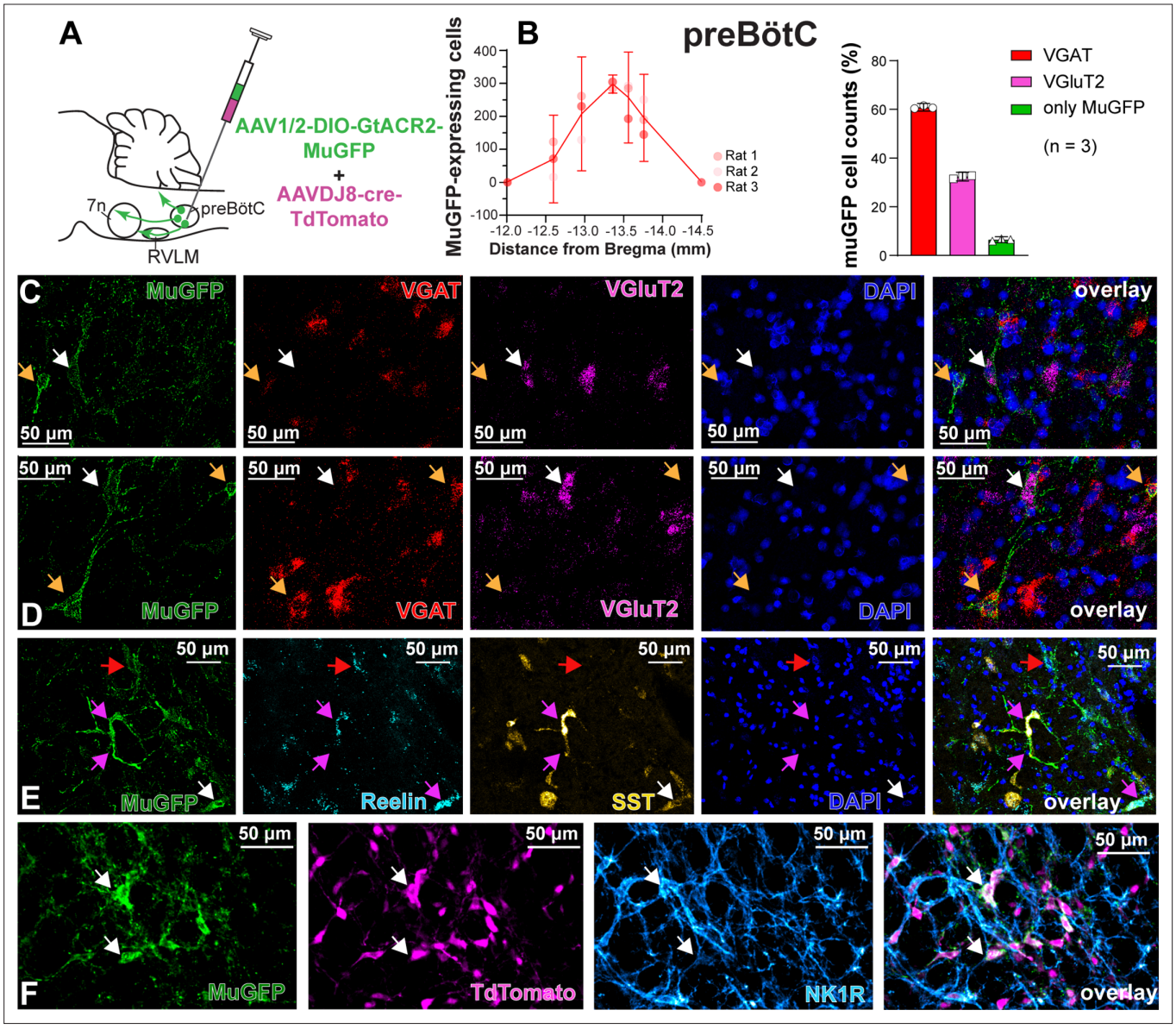

Figure 4. Excitatory and inhibitory pre-Bötzinger complex (preBötC) neurons are transduced by non-selective transfection of preBötC neurons. (**A**) Schematic diagram showing injection protocol for non-selective transduction of preBötC neurons. (**B**) Quantification of the total number of MuGFP-expressing neurons, plotted as the distance from Bregma (mm). The histograms show the number of transduced cells that co-expressed mRNA for *VGAT* or *VGluT2*. The results are presented as mean ± 95% CI. (**C–E**) In situ hybridization showing the co-expression of MuGFP (green), with mRNA for VGAT (red), VGluT2 (magenta), reelin (cyan), and somatostatin (SST) (yellow) in preBötC. Nuclei are labeled in blue (DAPI). The yellow arrows highlight *VGAT* neurons, the white arrows highlight *VGluT2* neurons, the red arrows highlight reelin neurons, and the pink arrows highlight reelin and SST neurons. (**F**) Immunohistochemistry showing that some neurons expressing MuGFP (green) and TdTomato (magenta) also express neurokinin-1 receptor (NK1R) (light blue). Co-localization is indicated by white arrows.

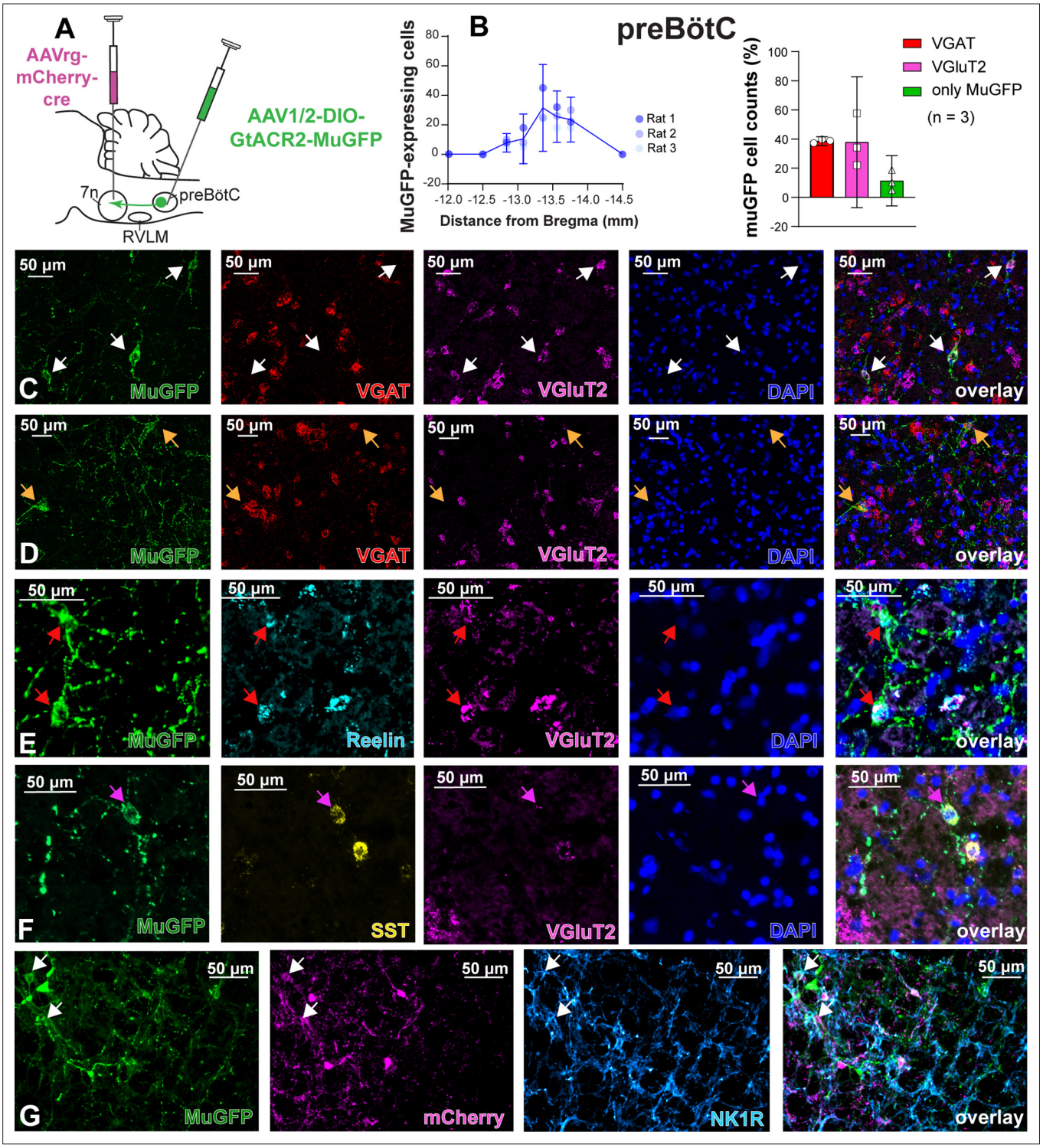

Figure 5. Excitatory and inhibitory pre-Bötzinger complex (preBötC) neurons are transduced by selective transduction of preBötC →7n neurons. (**A**) Schematic diagram showing the injection protocol for selective transduction of preBötC→7n neurons. (**B**) Quantification of the total number of MuGFP-expressing neurons, plotted as the distance from Bregma (mm). Note the slight trend toward a more caudal distribution. The histograms show the number of transduced cells that co-expressed mRNA for *VGAT* or *VGluT2*. The results are presented as mean ± 95% CI. (**C–F**) In situ hybridization showing the co-expression of MuGFP (green), with mRNA for VGAT (red), VGluT2 (magenta), reelin (cyan), or somatostatin (SST) (yellow) in preBötC→7n neurons. Nuclei are labeled in blue (DAPI). The yellow arrows highlight *VGAT* neurons, and the white arrows highlight *VGluT2* neurons, the red arrows highlight *reelin* neurons, and the pink arrows highlight *SST* neurons. (**G**) Immunohistochemistry showing that some neurons expressing MuGFP (green) and mCherry (magenta) also express neurokinin-1 receptor (NK1R) (light blue). Co-localization is indicated by white arrows.

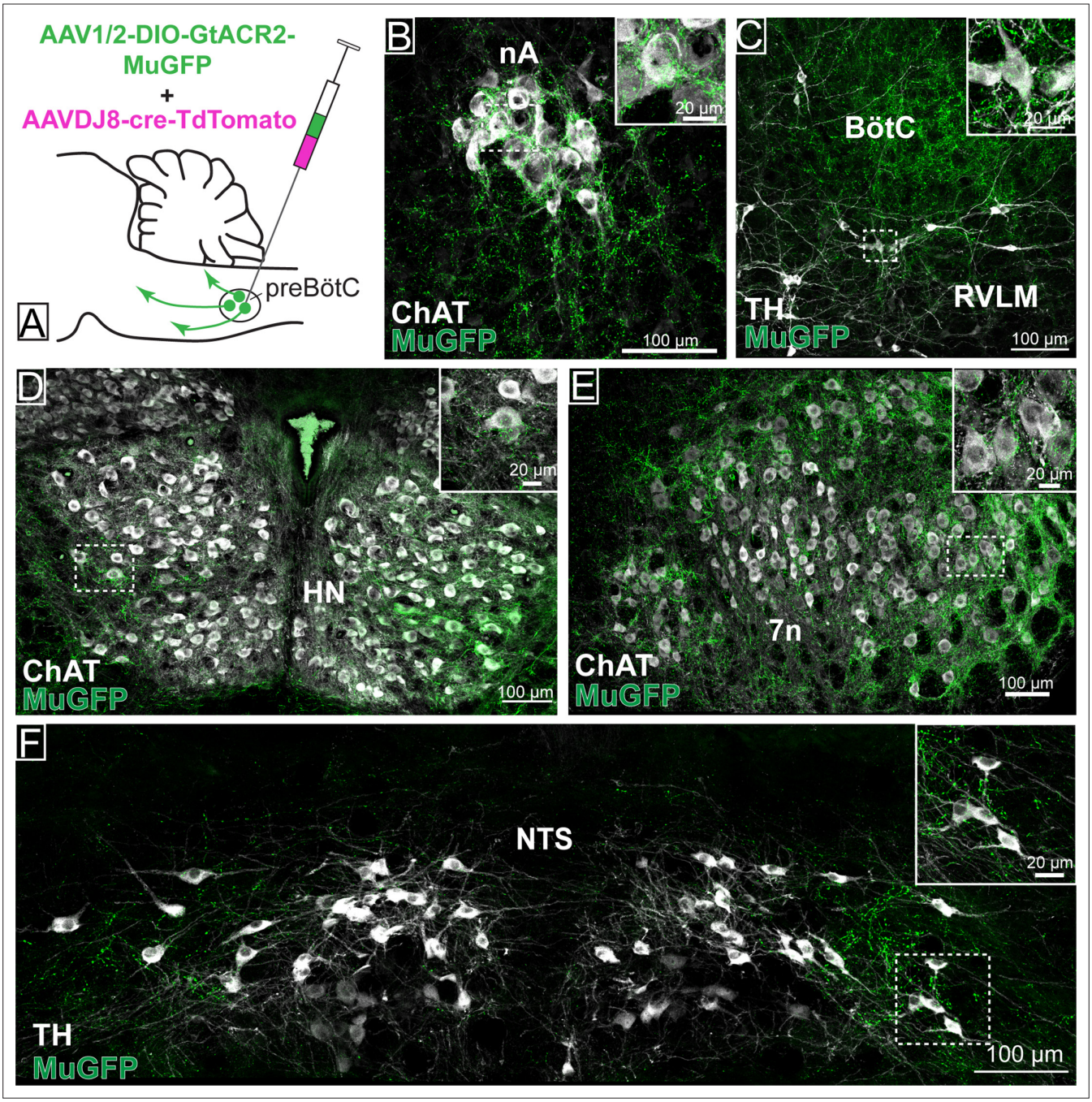

Figure 6. Distribution of GtACR2-MuGFP-expressing axons in multiple brainstem nuclei following the non-selective transduction of pre-Bötzinger complex (preBötC) neurons. (**A**) Schematic diagram showing the protocol for non-selective transduction of preBötC neurons. Confocal microscopy images demonstrate MuGFP expression in axon in the (**B**) nucleus ambiguus. (**C**) Rostral ventrolateral medulla and Bötzinger complex, (**D**) hypoglossal nucleus, (**E**) facial nucleus, and (**F**) nucleus of the solitary tract. Higher magnification images of the hashed-boxed regions are shown in the upper right corner of the lower magnification image. ChAT: choline acetyltransferase; TH: tyrosine hydroxylase.

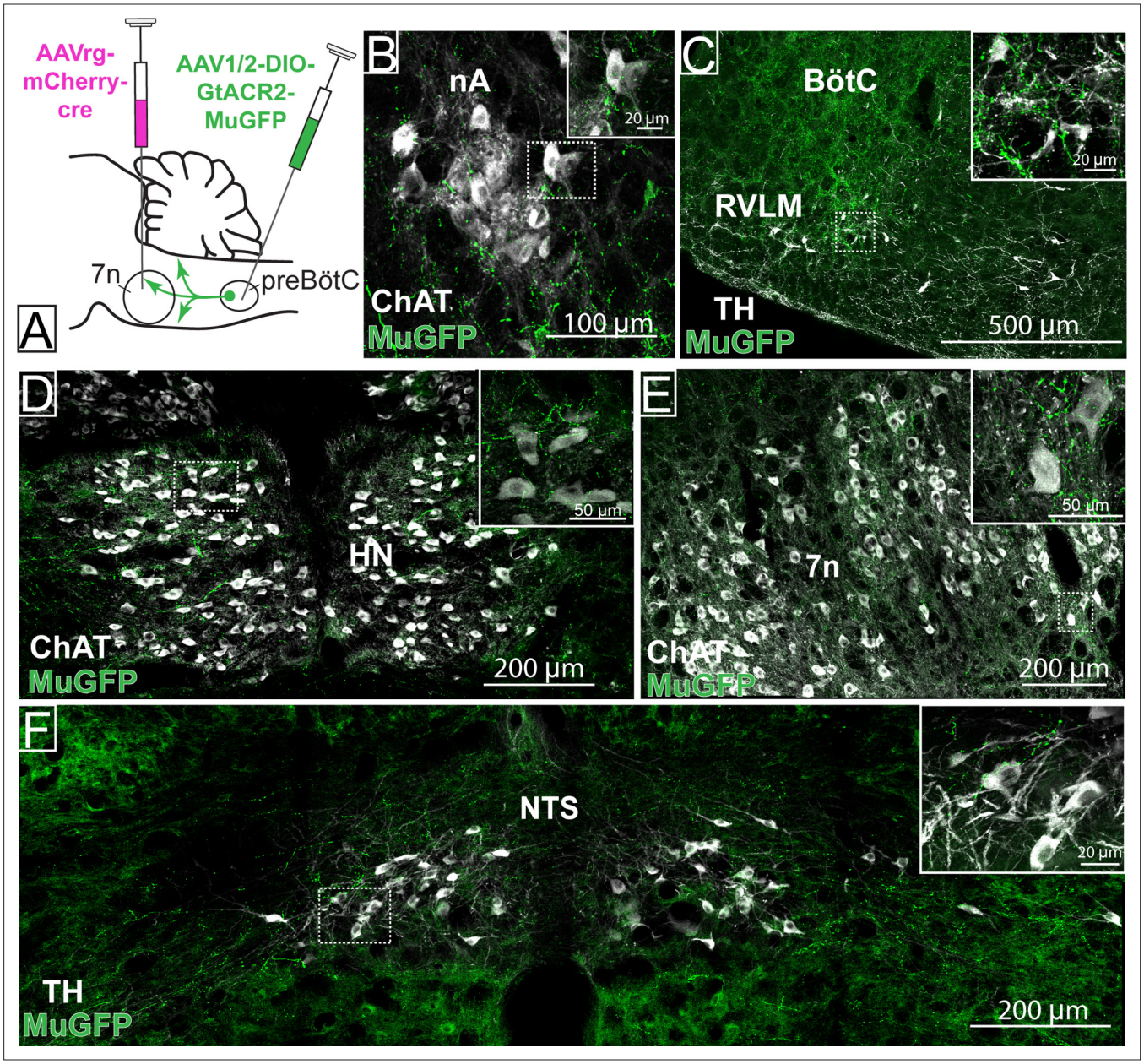

Figure 7. Distribution of selective pre-Bötzinger complex (preBötC)→7n GtACR2-MuGFP-expressing axonal projections. (**A**) Schematic diagram showing the injection protocol for selective transduction of preBötC→7n neurons. Confocal microscopy images highlighting the expression of MuGFP in axons in the (**B**) nucleus ambiguus; (**C**) rostral ventrolateral medulla and Bötzinger complex; (**D**) hypoglossal nucleus; (**E**) facial nucleus; and (**F**) nucleus of the solitary tract. Higher magnification images of the hashed-boxed regions are shown in the upper right corner of the lower magnification image. ChAT: choline acetyltransferase; TH: tyrosine hydroxylase.

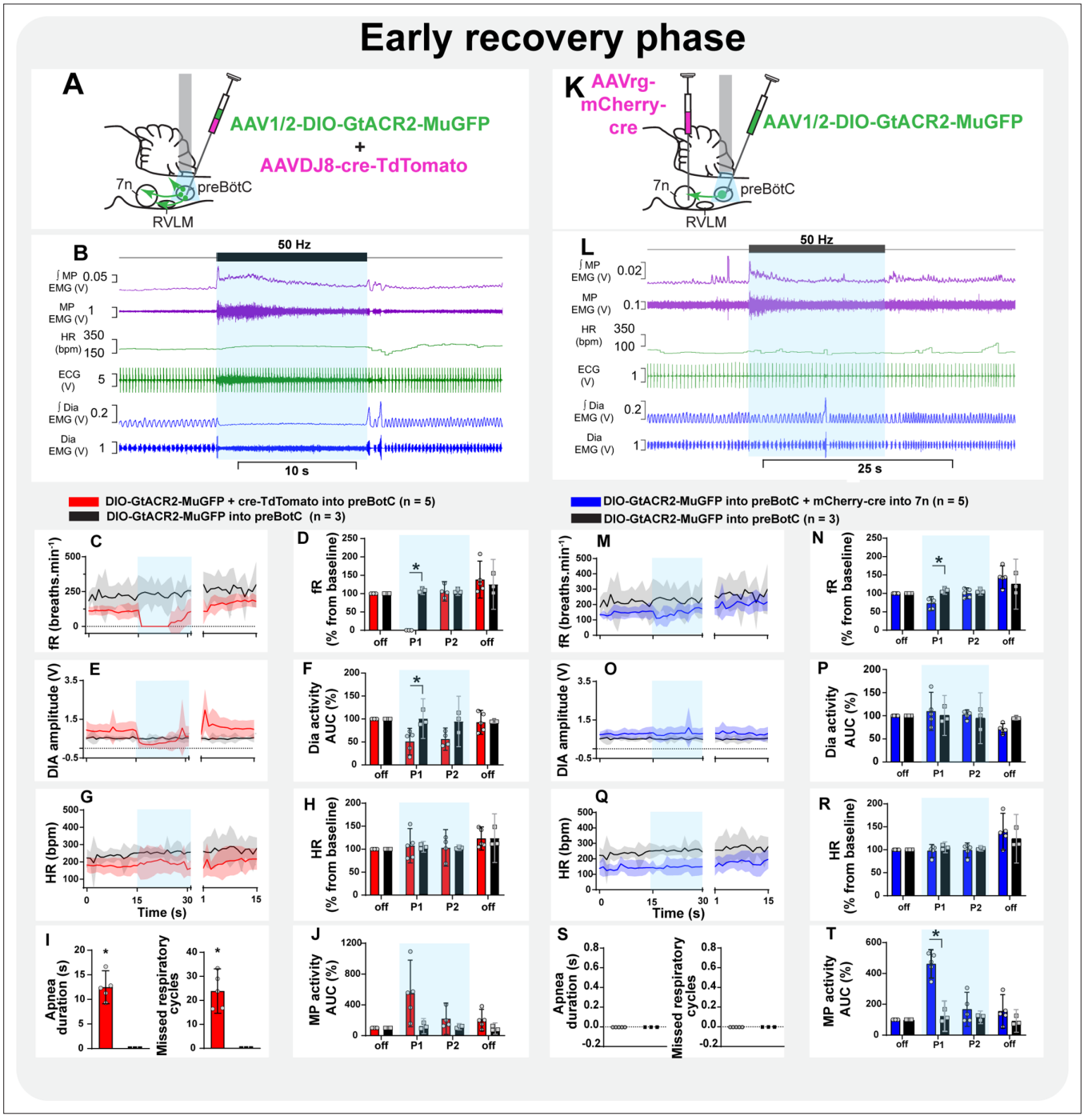

Figure 8. Effect of selective inhibition of pre-Bötzinger complex (preBötC)→7n neurons on mystacial pad (MP) activity is state-dependent. Schematic diagrams showing the injection protocols for non-selective transduction of preBötC neurons (**A**) and selective transduction of preBötC→7n neurons (**K**). Representative trace showing the integrated (∫) and raw MP EMG, heart rate (HR), electrocardiograms (ECG), and ∫ and raw diaphragm (Dia) EMG in the initial phase of reversal of ketamine/medetomidine anesthesia in rats with non-selective (**B**) and selective (**L**) preBötC neuron transduction. The period of photoinhibition is highlighted with the blue box. Group data showing mean (solid line) and 95% confidence intervals for (**C and M**) respiratory frequency - fR, (**E and O**) Dia amplitude, (**G and Q**) and HR (bpm) before, during, and after photoinhibition in non-selective (red), selective GtACR2 expressing (blue), and control (black) rats. Histograms showing group data for the effect of photoinhibition of preBötC on respiratory and cardiovascular parameters (**D and N**) fR, (**F and P**) Dia amplitude, (**H and R**) HR, (**I and S**) apnea duration and number of missed respiratory cycles, and (**J and T**) MP activity.; P1 and P2 refer to the initial period of photoinhibition. Group data are presented as mean ± 95% CI; unpaired t-test or nonparametric Mann-Whitney test with multiple comparisons using the Bonferroni-Dunn method, *p<0.05. The photoinhibition of preBötC neurons is depicted by blue shading. The effects of non-selective and selective photoinhibition of preBötC in ketamine/medetomidine-anesthetized rats are shown in ***Figure 8—figure supplement 1***.

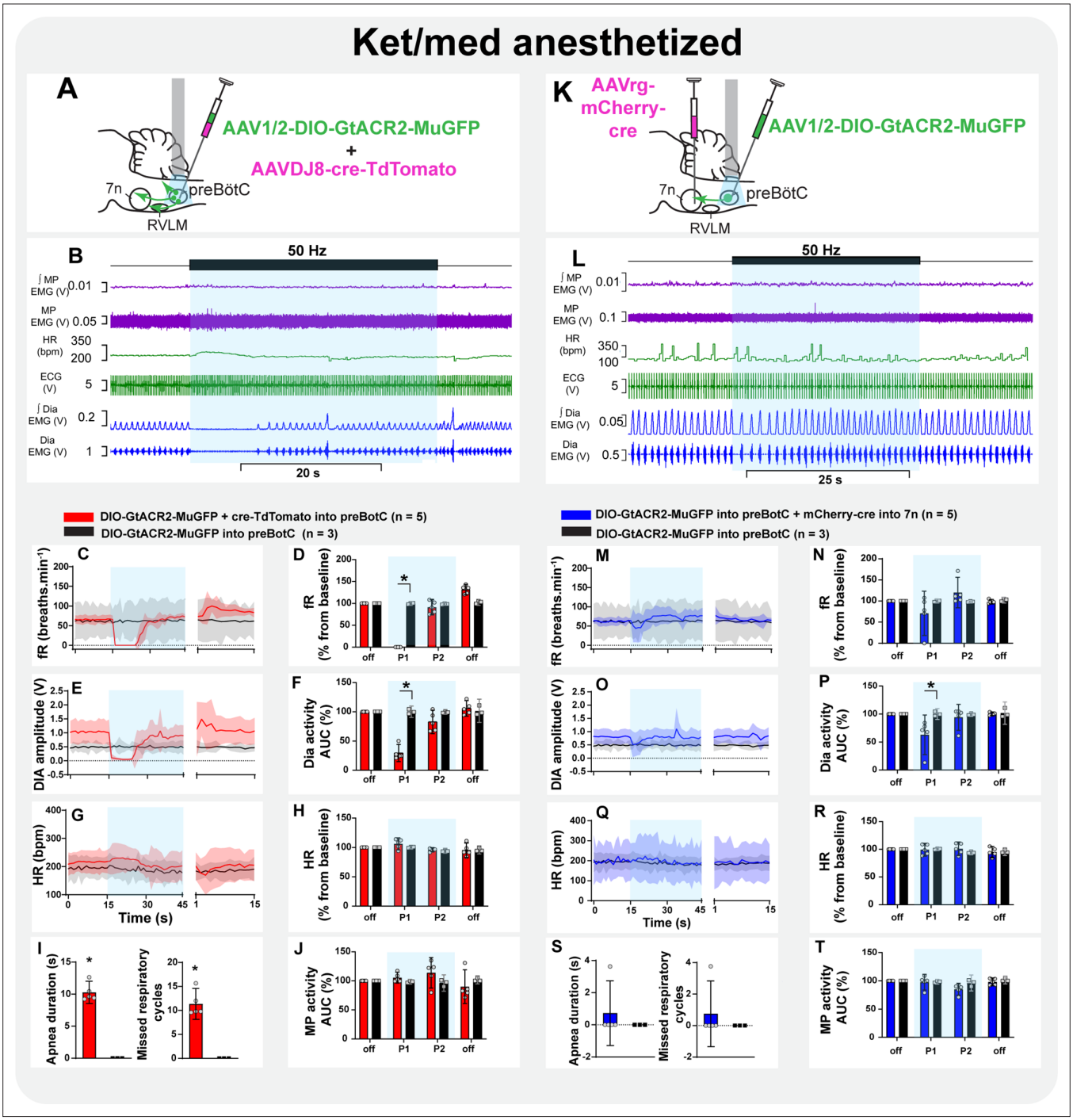

Figure 8—figure supplement 1. Effect on non-selective and selective inhibition of pre-Bötzinger complex (preBötC) on mystacial pad (MP) activity under ketamine/medetomidine anesthesia. Schematic diagrams showing the injection protocols for non-selective transduction of preBötC neurons (**A**) and selective transduction of preBötC→7n neurons (**K**). Representative trace showing the integrated (∫) and raw MP EMG, heart rate (HR), electrocardiograms (ECG), and ∫ and raw diaphragm (Dia) EMG in ketamine/medetomidine-anesthetized rats with non-selective (**B**) and selective (**L**) transduction. The period of photoinhibition is highlighted with the blue box. Group data showing mean (solid line) and 95% confidence intervals for (**C and M**) respiratory frequency - fR, (**E and O**) Dia amplitude, (**G and Q**) and HR (bpm) before, during, and after photoinhibition in non-selective (red), selective GtACR2 expressing (blue) and control (black) rats. Histograms showing group data for the effect of photoinhibition of preBötC on respiratory and cardiovascular parameters (**D and N**) fR, (**F and P**) Dia amplitude, (**H and R**) HR, (**I and S**) apnea duration and number of missed respiratory cycles, and (**J and T**) MP activity; P1 and P2 refer to the initial period of photoinhibition. Group data are presented as mean ± 95% CI; unpaired t-test or nonparametric Mann-Whitney test with multiple comparisons using the Bonferroni-Dunn method, *p<0.05. The photoinhibition of preBötC neurons is depicted by blue shading.

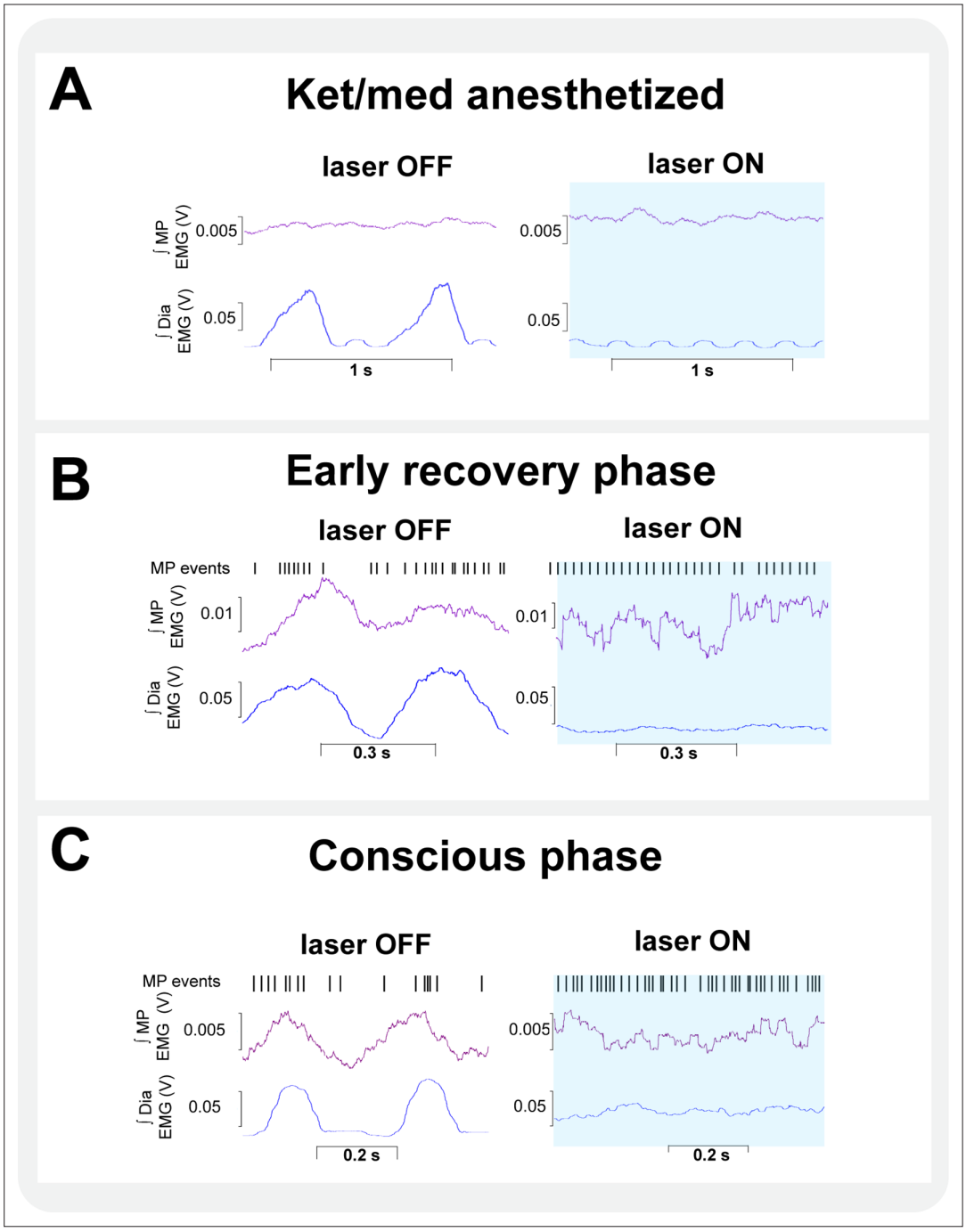

Figure 8—figure supplement 2. Effects of non-selective inhibition of pre-Bötzinger complex (preBötC) on the mystacial pad (MP) and diaphragm activity in different state conditions. Higher temporal resolution recordings showing MP bursts as events, and triggered averages of integrated (∫) MP and ∫ Dia EMG during the baseline period and during the beginning of non-selective photoinhibition of preBötC neurons. Photoinhibition was performed in three different conditions. (**A**) Under ketamine/medetomidine anesthesia, MP activity was minimal and non-rhythmic during baseline, and was not affected by the apnea. (**B**) During the early recovery phase from anesthesia, photoinhibition of non-selectively transduced preBötC neurons induced apnea and interrupted inspiratory-related MP activity, which increased and become tonic for the apnea period. (**C**) After the animals were conscious and freely behaving, the non-selective photoinhibition also interrupted the inspiratory-related MP activity, which became increased and tonic. The period of photoinhibition is highlighted with the blue box.

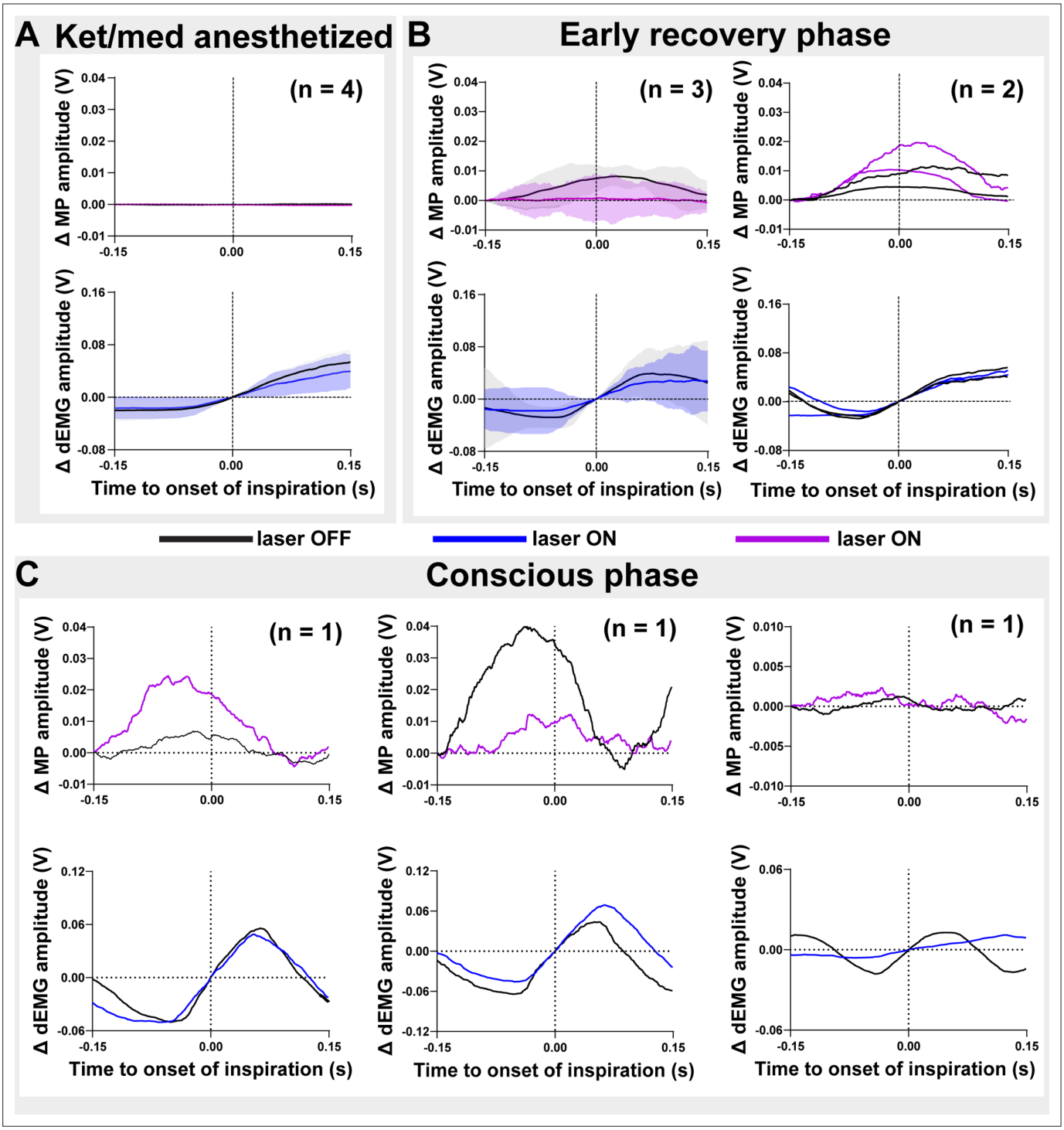

Figure 8—figure supplement 3. Effects of selective inhibition of pre-Bötzinger complex (preBötC)→7n neurons on the mystacial pad and diaphragm activity in different state conditions. Event-triggered average showing the magnitude of respiratory-related modulation of mystacial pad (MP) amplitude in the 150 ms before and after the onset of inspiration during baseline and during the beginning of photoinhibition. The averages were triggered by the rapid rise of the diaphragm (diaphragm electromyography [dEMG]) amplitude that occurs at the beginning of inspiration. The averaging period comprised 5–8 respiratory cycles. Group data show the inhibition of preBötC→7n in three different state conditions: (**A**) ketamine/medetomidine anesthesia, (**B**) during the early-recovery phase after reversal of anesthesia with atipamezole, and (**C**) after the regaining of consciousness. Data are presented as mean ± 95% CI.

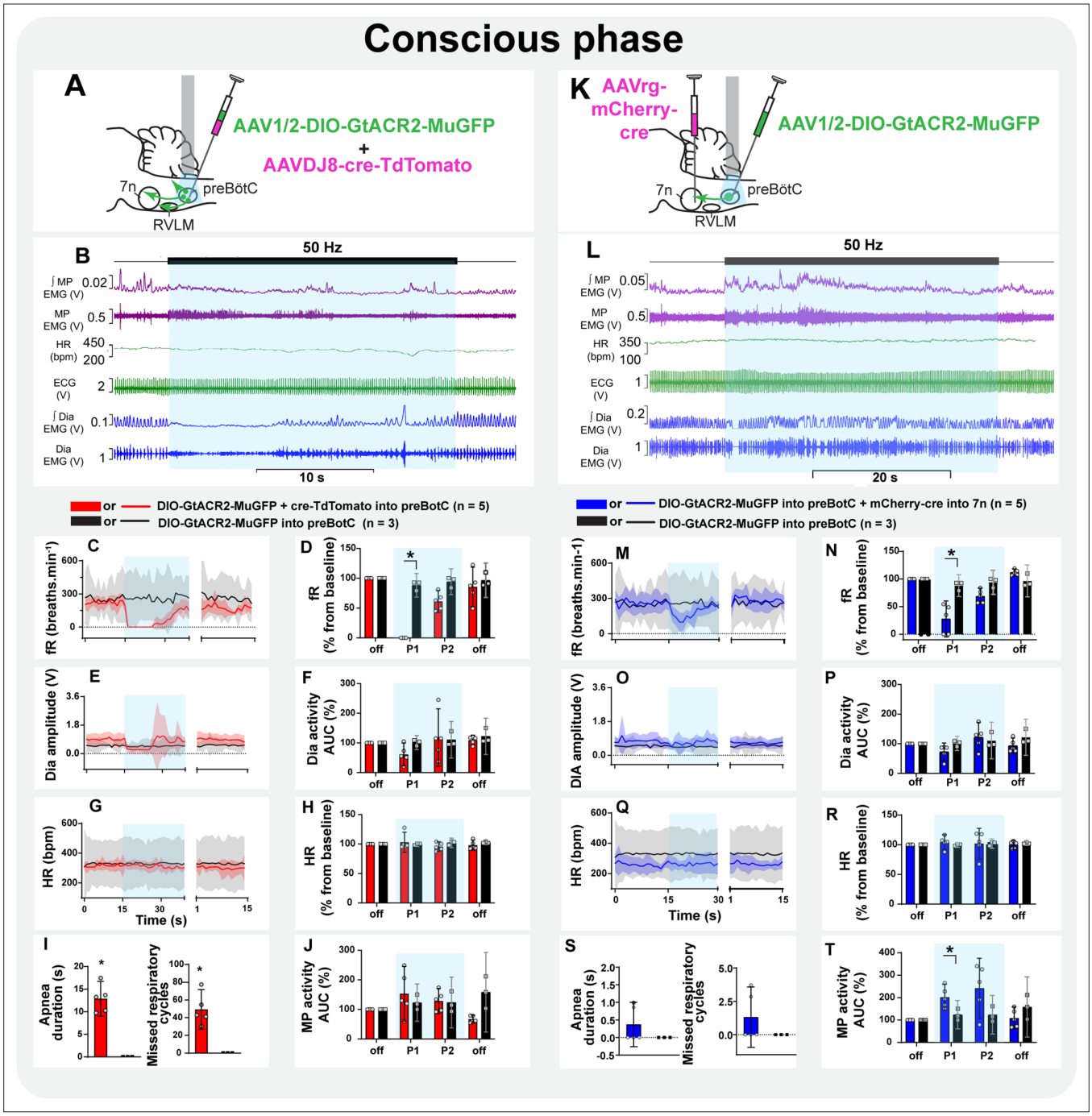

Figure 9. Inspiratory-related activity of mystacial pad is interrupted by the selective inhibition of pre-Bötzinger complex (preBötC) to 7n neurons in conscious rats. Schematic diagrams showing the injection protocols for non-selective transduction of preBötC neurons (**A**) and selective transduction of preBötC→7n neurons (**K**). Representative trace showing the integrated (∫) and raw mystacial pad (MP) EMG, heart rate (HR), electrocardiograms (ECG), and ∫ and raw diaphragm (Dia) EMG after recovery from ketamine/medetomidine anesthesia in rats with non-selective (**B**) and selective (**L**) preBötC neuron transduction. The period of photoinhibition is highlighted with the blue box. Group data showing mean (solid line) and 95% confidence intervals for (**C and M**) respiratory frequency - fR, (**E and O**) Dia amplitude, (**G and Q**) and HR (bpm) before, during, and after photoinhibition in non-selective (red), selective GtACR2 expressing (blue) and control (black) rats. Histograms showing group data for the effect of photoinhibition of preBötC on respiratory and cardiovascular parameters (**D and N**) fR, (**F and P**) Dia amplitude, (**H and R**) HR, (**I and S**) apnea duration and number of missed respiratory cycles, and (**J and T**) MP activity; P1 and P2 refer to the initial period of photoinhibition. Group data are presented as mean ± 95% CI; unpaired t-test or nonparametric Mann-Whitney test with multiple comparisons using the Bonferroni-Dunn method, *p<0.05. The photoinhibition of preBötC neurons is depicted by blue shading.